# Investigation of atmospheric piston phase variations and the effects on coherent systems under extremely low SNR

19 November 2014

Dr. Skip Williams

Air Force Research Laboratory

*Integrity ★ Service ★ Excellence*

# Acknowledgements


**6.1 AFOSR Funded Team Members**

- **AFRL/RDS: Jeremey Bos, Rao Gudimetla**
- **Boeing: Brandoch Calef**
- **Jet Propulsion Laboratory: Bijan Nemati, Michael Shao, Hanying Zhou**

**6.2 AFRL/RD Funded Contributors (SimISAL & Lab Validation)**

- **The Optical Science Company: N. Steinhoff, G. Tyler**
- **Boeing: David Gerwe, Tom Kelecy, Andrew Whiting**
- **Schafer: David Briscoe**

# Inverse Synthetic Aperture LADAR (ISAL) Overview

**Present Capability**

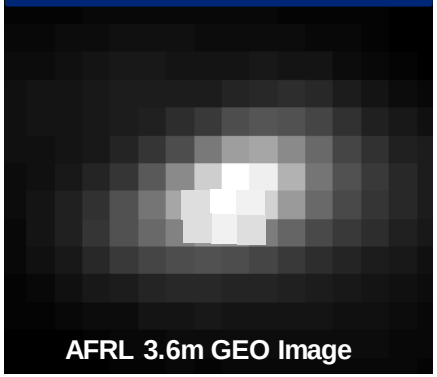

AFRL 3.6m GEO Image

- **Next Generation GEO Imaging**
  - Affordable techniques for imaging (radar and/or optical) of objects in deep space orbits"

**ISAL Capability**

Simulated ISAL GEO Image

- **ISAL Imaging**
  - As object and observer move relative to each other the series of returns (pulses) fills in the range/cross-range Fourier plane,
  - Coherent detection requires local oscillator and coherent waveform
  - Image resolution from bandwidth & angular diversity

**ISAL GEO Imaging**

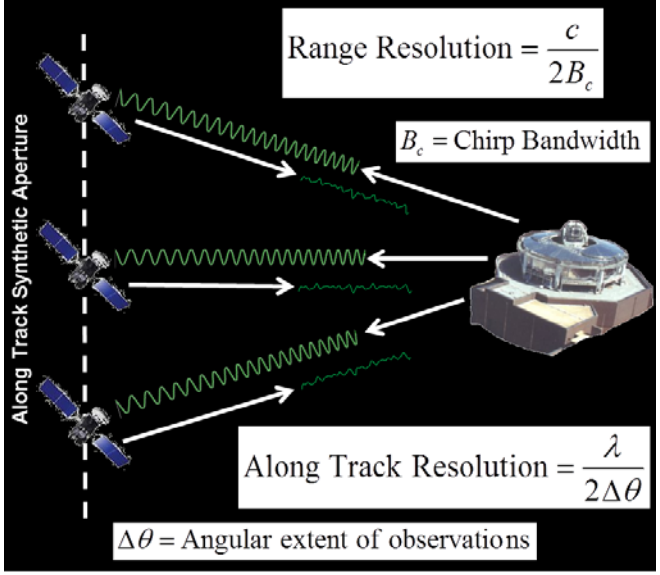


**Atmospheric piston corrupts range & cross-range phase information**

# Overview of ISAL Technical Elements

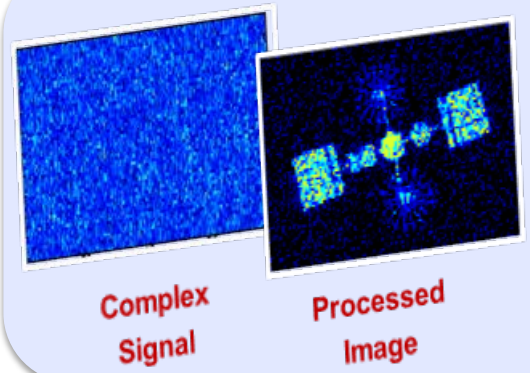


## Image Processing

- Atmosphere√
- SNR
- Resolution
- Autofocus√

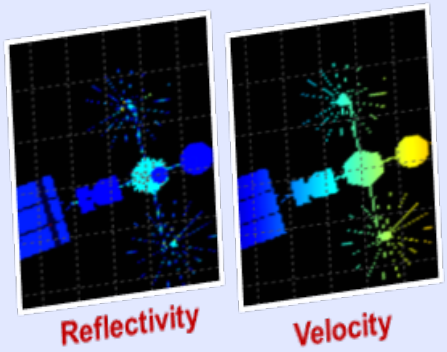


## Target

- Active & passive cross sections
- Rotation rate
- Articulation
- Vibration

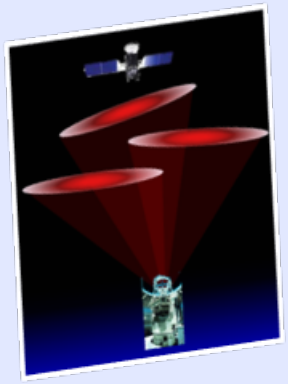

## Electro Optical (EO) Systems

- Telescope & optical bench
- Laser and tracking jitter
- Transmit/Receive switching
- Atmospheric compensation

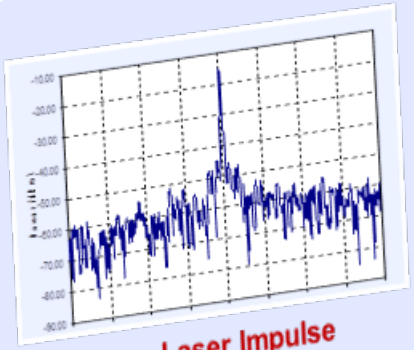


## Transceiver

- Transmitter power
- Chirped waveforms
- Phase errors
- Heterodyne detection efficiency
- Laser beam quality

**AFOSR tasks focuses on image processing**

# Inverse Synthetic Aperture LADAR (ISAL) Image Processing SNR Derivation

- **Detector output is given by**

$$i(t) = \frac{q_e \eta_d}{\tau_p}\left[\frac{N_{LO}}{2} + s(t)\right]$$

**where *s(t)* is the ISAL signal given by**

$$s(t) = \sqrt{\eta_h N_{LO} N_s}\int_{-z_1}^{z_1} \cos\left\{\frac{2(z-\acute{z})}{c}[\omega_0 + 2\beta(t-\tau_0)] - \frac{4\beta(z^2-\acute{z}^2)}{c^2}\right\} dz$$

- **Signal to noise ratio is defined as**

$$\text{SNR} = \frac{E\left[|S(f)|^2\right]}{\sigma_{|S(f)|^2}}$$

**Signal at each range bin**

**Signal std. deviation at each range bin**

$$\text{SNR} = \frac{N_s}{\sqrt{\frac{(\eta_d N_{LO}) + (\eta_d N_{LO})^2 + 2(\eta_d N_{LO})^2 \eta_h N_s + 4\eta_d^2 \eta_h N_{LO} N_s + \eta_d^4 \eta_h^2 N_{LO}^2 N_s^2}{\eta_d^4 \eta_h^2 N_{LO}^2 N_s^2}}} \sim \frac{N_s}{N_s + \frac{1}{\eta_{det}}}$$

**SNR limited to 1 due to speckle for ISAL**

$q_e$ - electron charge
$\eta_d$ - quantum efficiency
$\eta_h$ - heterodyne efficiency
$\eta_{det} \sim \eta_d * \eta_h$
$\tau_p$ - chirp period
$N_{LO}$ - LO photons over pulse
$N_s$ - signal photons over pulse
$z$ - range
$\acute{z}$ - LO & signal path difference
$c$ - speed of light
$\omega_0$ - laser center frequency
$\beta$ – chirp rate (Hz/s)
$\tau_0$ - round trip time
$S(f)$ - FFT of $s(t)$

# SimISAL
# An in-House M&S Tool

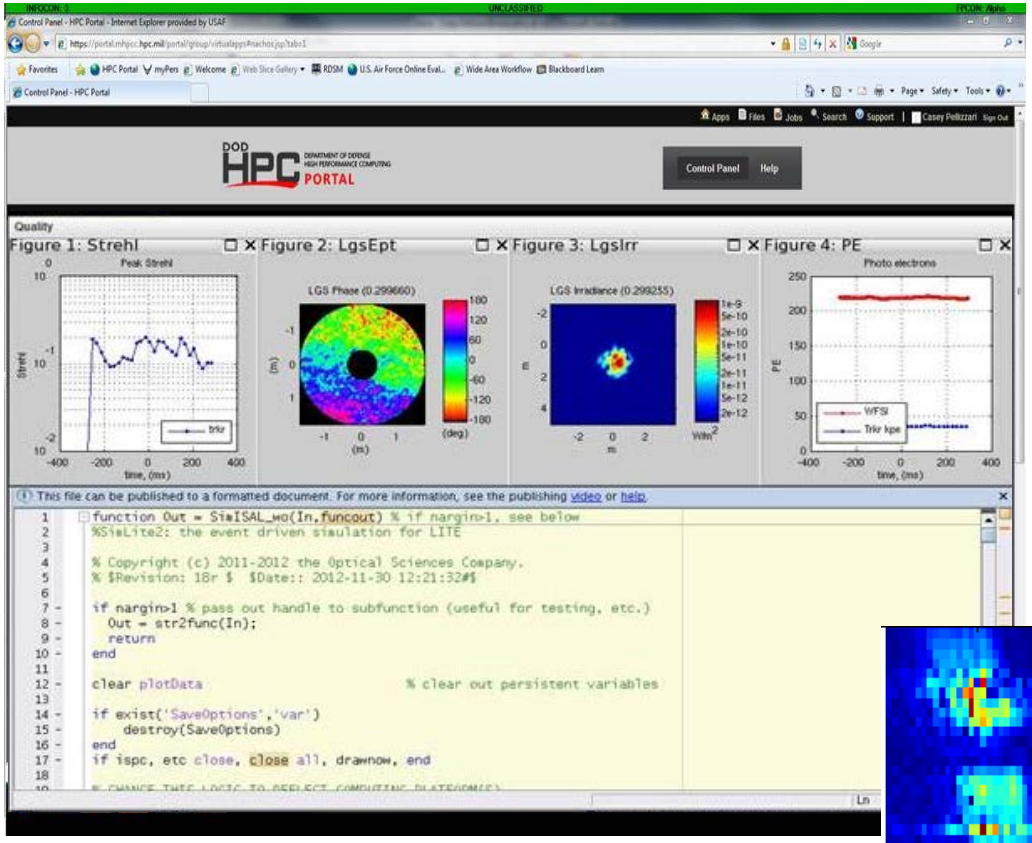


- First fully integrated ISAL M&S tool
  - 100% Physics based simulation
- Modular design allows for independent verification, tractable modifications & simplified use
- HPC allows for 60X speed increase enabling simulation based design and validation
- *Proc. SPIE 8877*, Unconventional Imaging and Wavefront Sensing 2013

Simulations of generic object as a function of image degradation sources

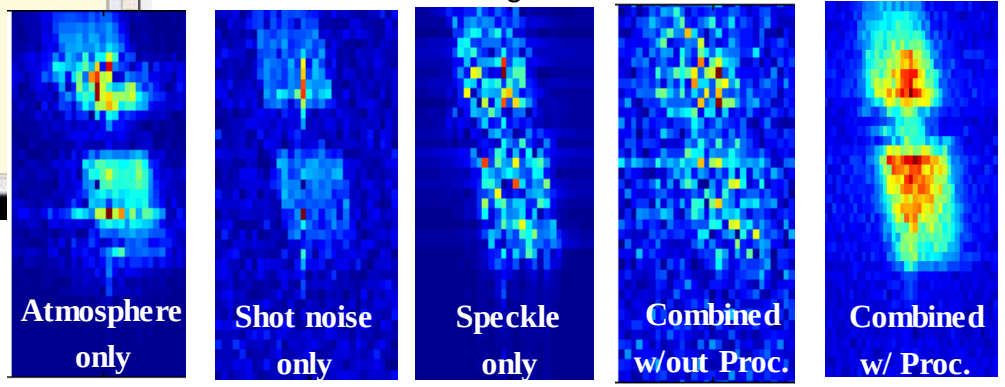


**Dec 2012 – Deployed via DoD High Performance Computing Program**

# Wave-Optics Overview
# Active Illumination

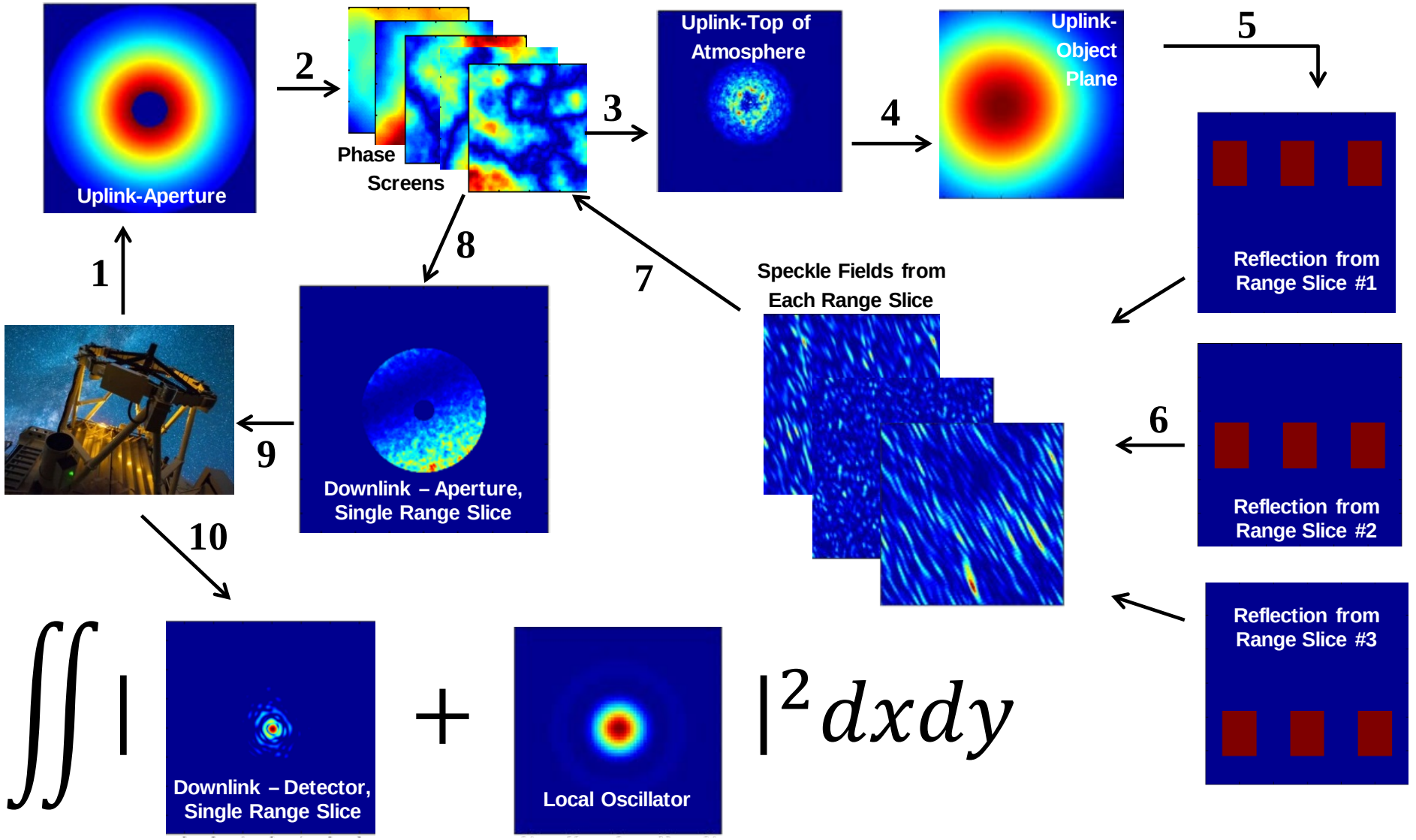

# Wave-Optics Overview
# AO System

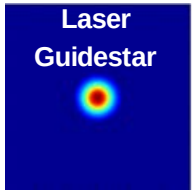


7

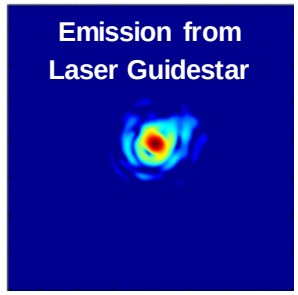


9

8

2, 10

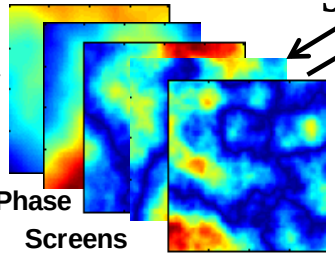


11 Laser Guidestar Phase

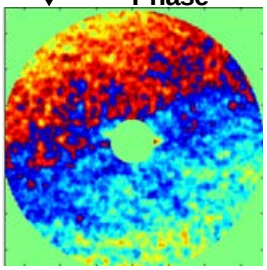

3

Passive Irradiance

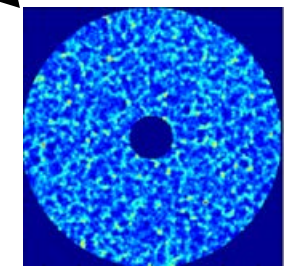

1

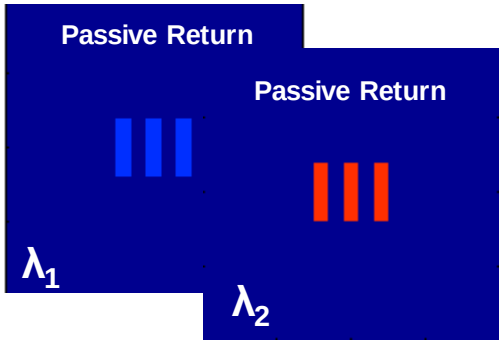


12

FSM OPD

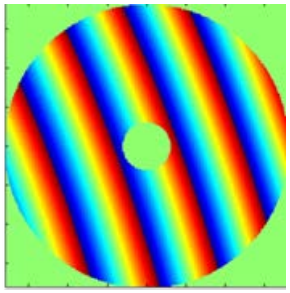

4

DM OPD

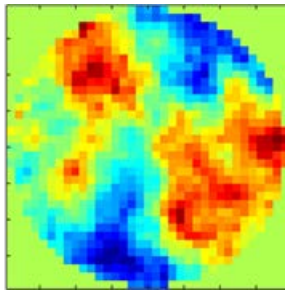

6

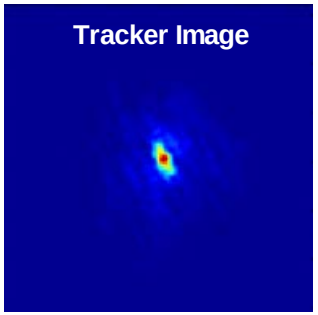


5,
13

14

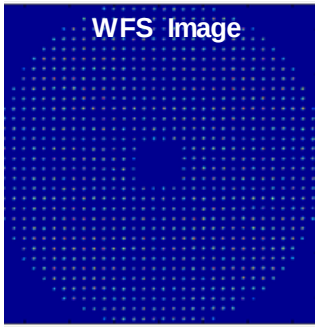

# Wave-Optics Output

$$I(t) = \frac{E_{LO}^2}{2} + \alpha\sqrt{\eta_h}\, E_{LO}\, E_s\, \mathrm{Re}\left(\int_{-z_1}^{z_1} o(z)\, \exp\left\{\left(z - \frac{c}{2}\tau_d\right)\frac{2}{c}[\omega_0 + 2\beta(t-\tau_0)] - \frac{4\beta z^2}{c^2} + \beta{\tau_d}^2\right\} dz\right),$$

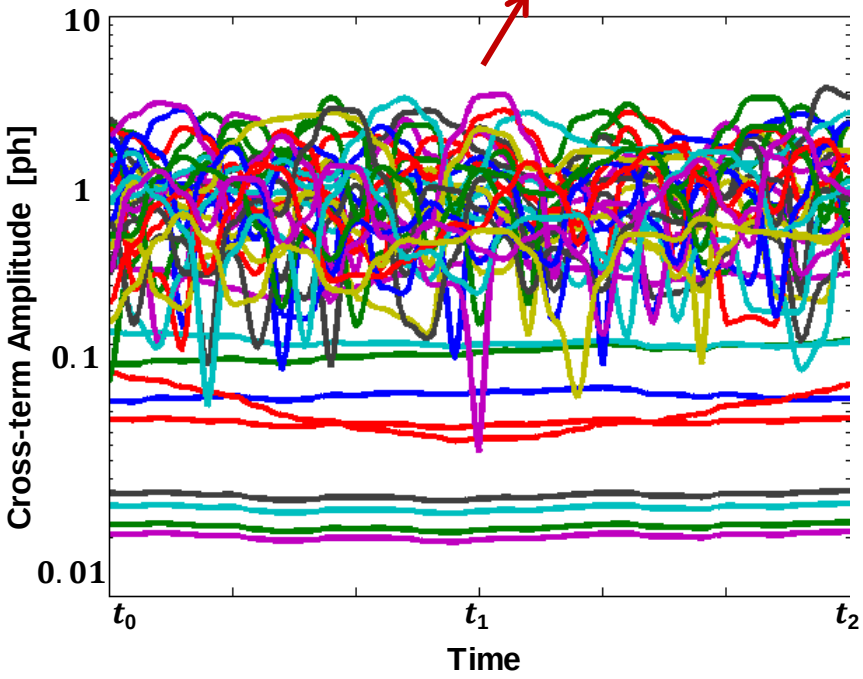


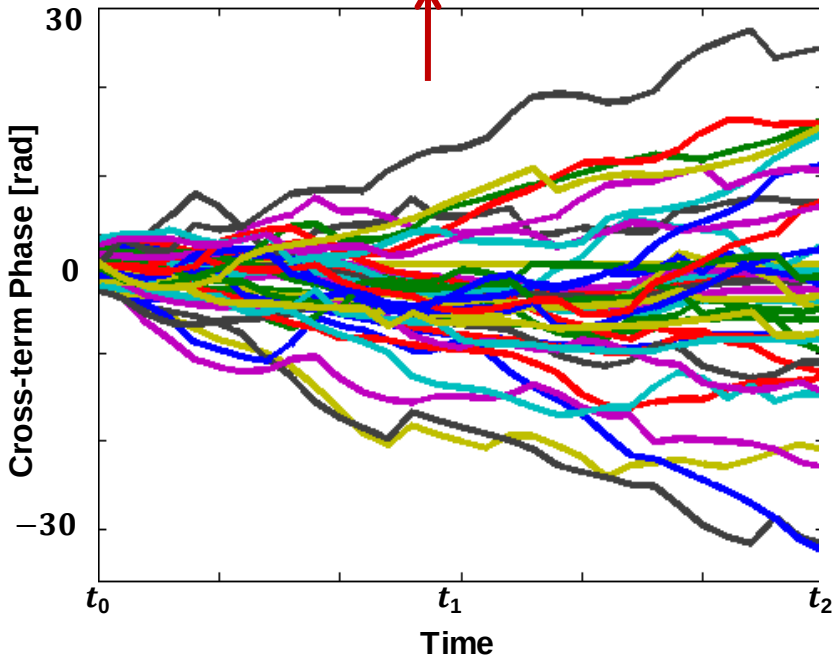


**Amplitude & phase for each cross term are the key wave-optics output**

# Detector Output

- **The detector module uses the wave-optics output to generate detected signal**
  - Requires interpolating wave-optics output to MHz rate
  - Output in one continuous data stream from all pulses

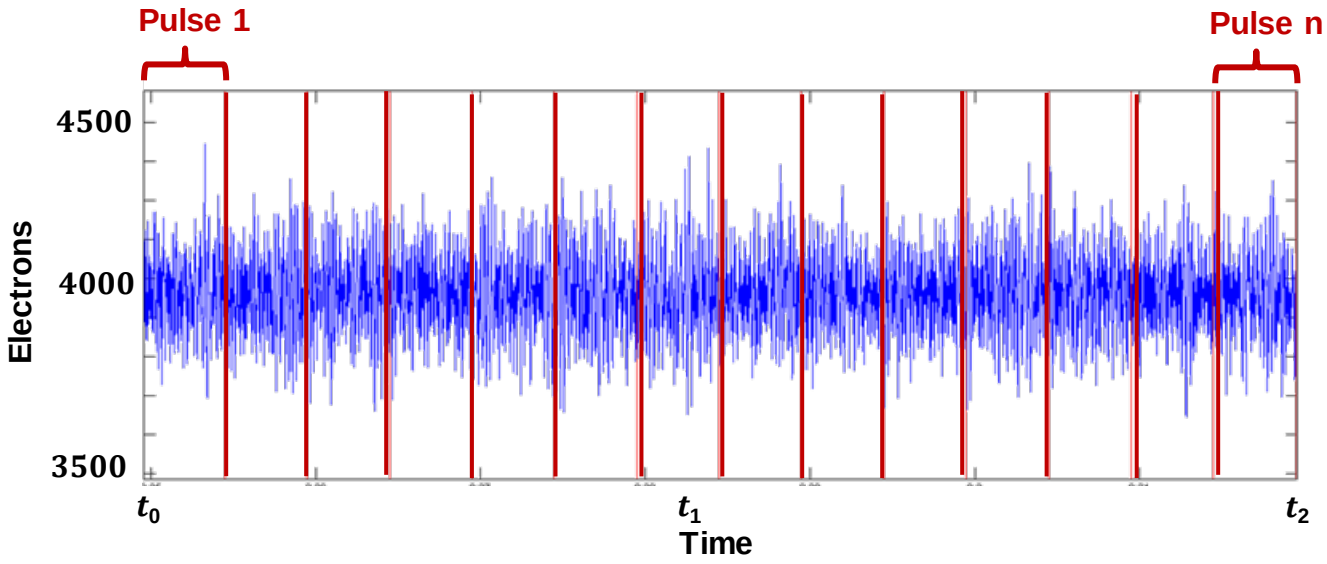


**Realistic detector current gets saved to disk**

# Pre-Processing

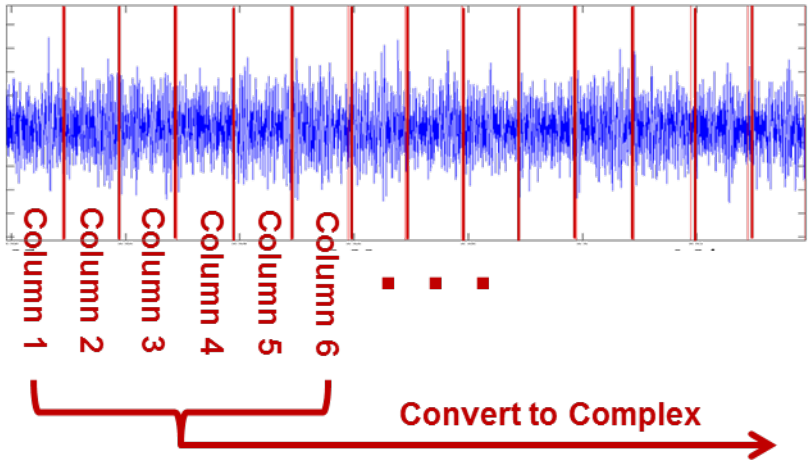


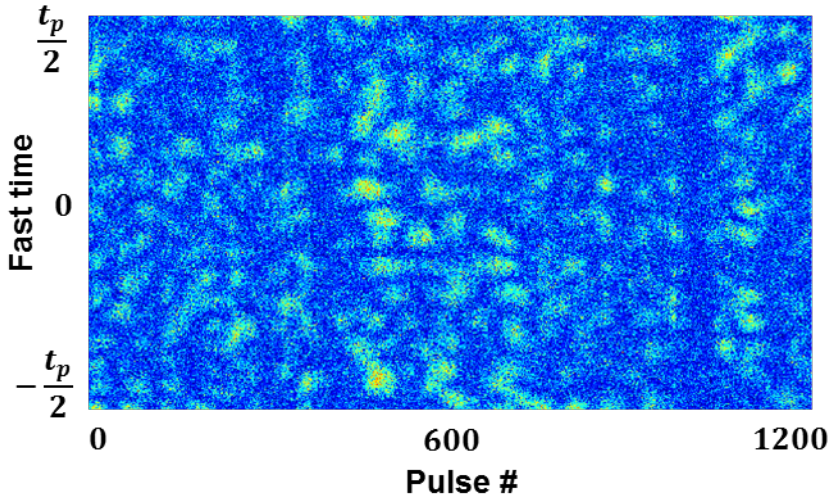


- Preprocessing splits the detector output into pulses
- A Hilbert transform is used to generate the imaginary component from the measured real component

Raw complex ISAL Data represents spatial frequency information in range & cross-range dimensions

**Detector output must be split into a fast-slow time array**

# Example Image

- The best way to verify the system as a whole is to produce a test image
- Example Image parameters

| Parameter | Value |
|---|---|
| Laser wavelength | 1064nm |
| Laser power | 2kW |
| Pulse repetition frequency (PRF) | 200Hz |
| Duty cycle | 100% |
| Wave-optics sample rate | 400Hz |
| Simulation time | 8s |
| Aperture diameter | 4m |
| Object rotation rate | 1μrad/s |
| Object OCS | $10\mathrm{m}^2/\mathrm{sr}$ |
| Object zenith angle | 45 degrees |
| Detector sample rate | 100kHz |
| Number of detectors | 2 |
| Quantum efficiency | 0.5 |
| A/D bits | 8 |

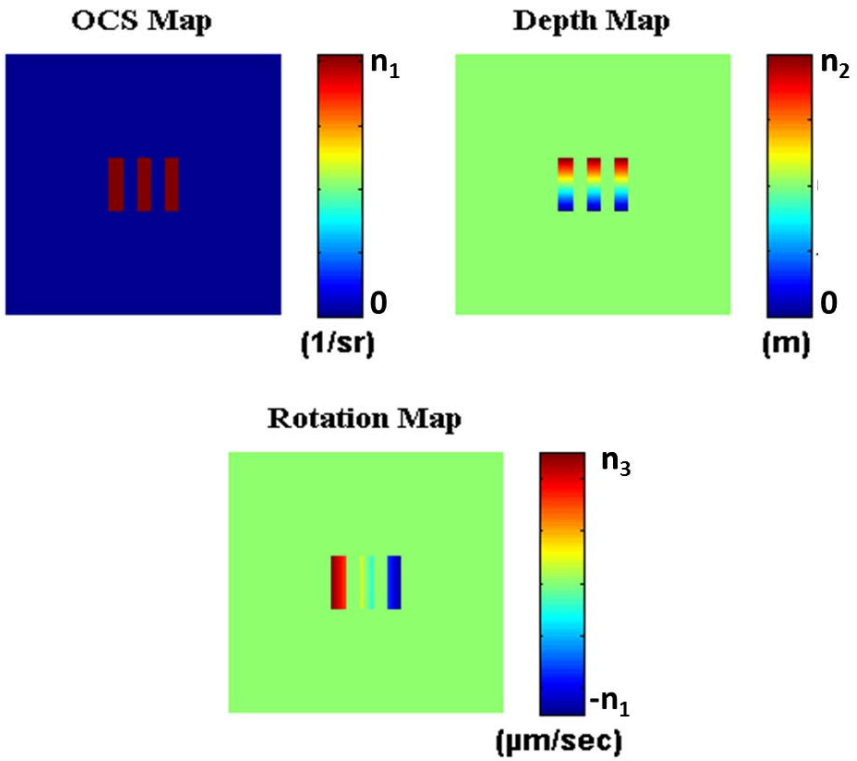

# Image Processing Autofocus

- **Atmospheric piston will corrupt the phase information for each laser return**
  - Autofocus algorithms adjust phase to maximize image contrast
  - Baseline approach is Phase Gradient Autofocus (PGA)
  - PGA consists of 4 steps
    - Centering
    - Windowing
    - Phase estimation
    - Iterative correction to minimize entire aperture phase error
  - Performance is limited by signal strength

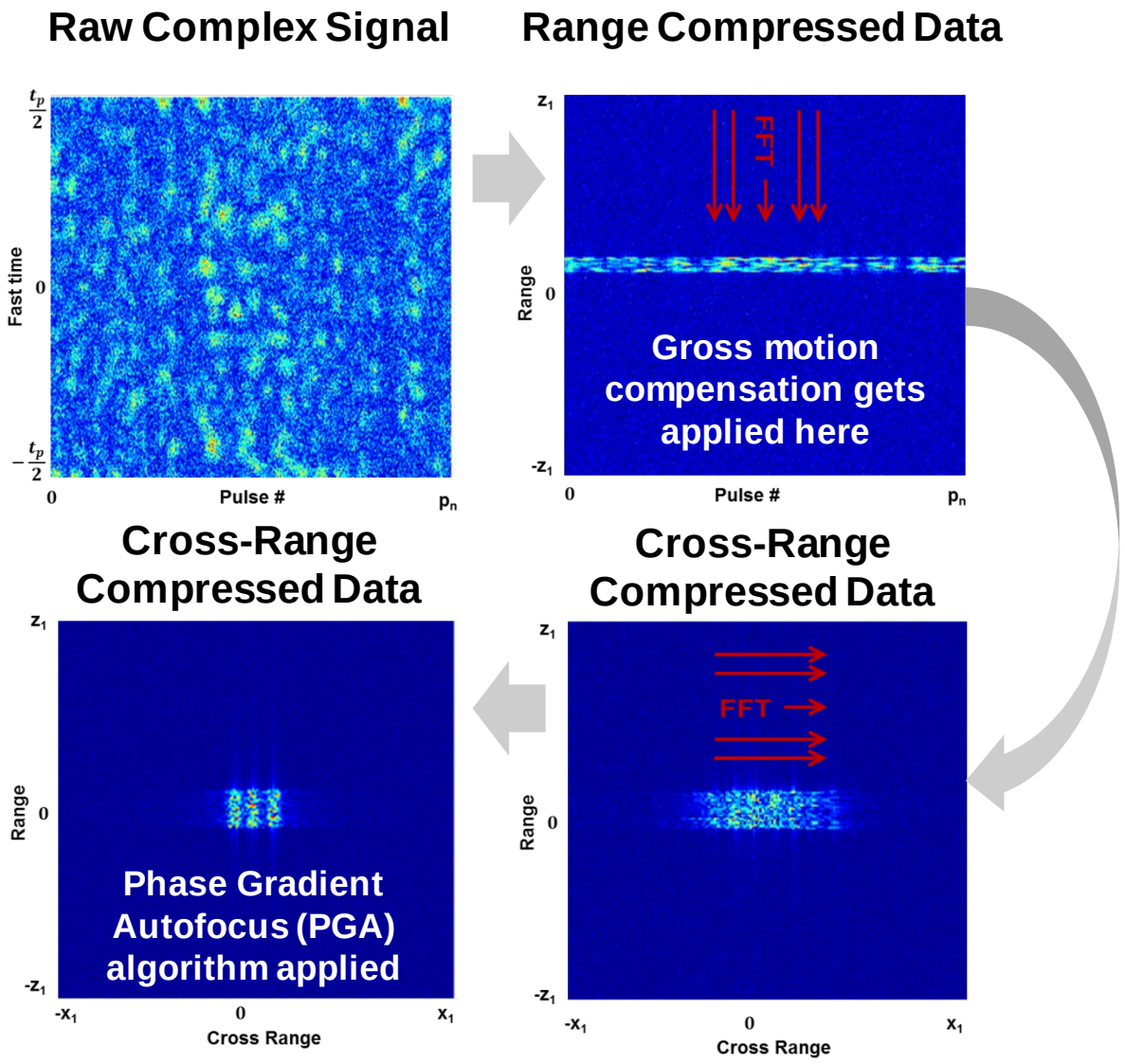

# PGA Detailed View

- The PGA algorithm may be summarized as follows:
  - $h(k,n)$ is the target reflectance at range *k* and cross-range *n*
  - $g(k,m)$ is the FFT of $\boldsymbol{g}$ with respect to *n*, evaluated at pulse *m*
  - $\varphi_i(m)$ *is the phase perturbation at pulse m, i.e., piston phase*
  - $\bar{g}(k,m) = e^{l\varphi_m} g(k,m)$ is the range-compressed, phase corrupted signal
- With these definitions, the estimate of the pulse-to-pulse phase change over *N* range bins is

$$\Delta\varphi(m) = \arg \sum_{k=1}^{N} \bar{g}(k,m+1)\bar{g}^*(k,m) - \text{mean}\ (\Delta\varphi)$$

- The estimate of the residual phase at pulse m is

$$\hat{\varphi}^{PGA}(m) = \sum_{i=1}^{m} \Delta\varphi(i)$$

- PGA applies the phase estimate repeatedly to minimize $\hat{\varphi}^{PGA}$ until convergence is obtained.

# PFA Autofocus Performance Limitations (CNR~1)

- ISAL M&S tool enables
  - Derive Autofocus requirements
  - Baseline PGA approach
  - Evaluate improved methods

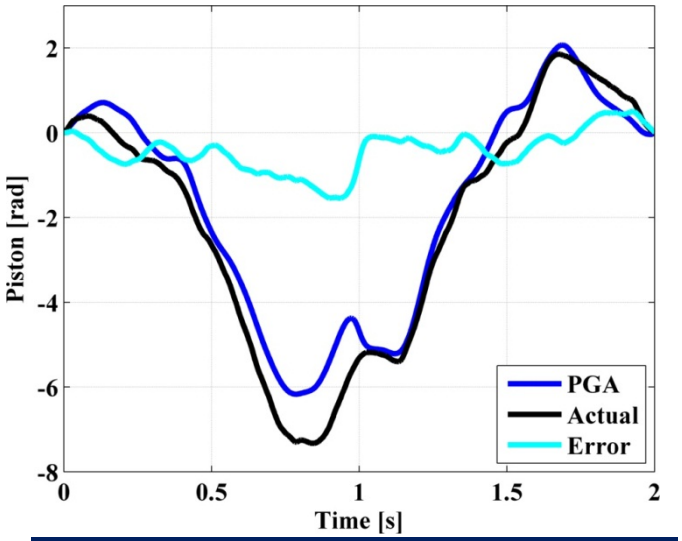


Simulated atmospheric piston-phase, PGA retrieval, and error

$$CNR = \frac{Signal\ Mean}{Noise\ Mean} \approx \eta_{det} N_s$$

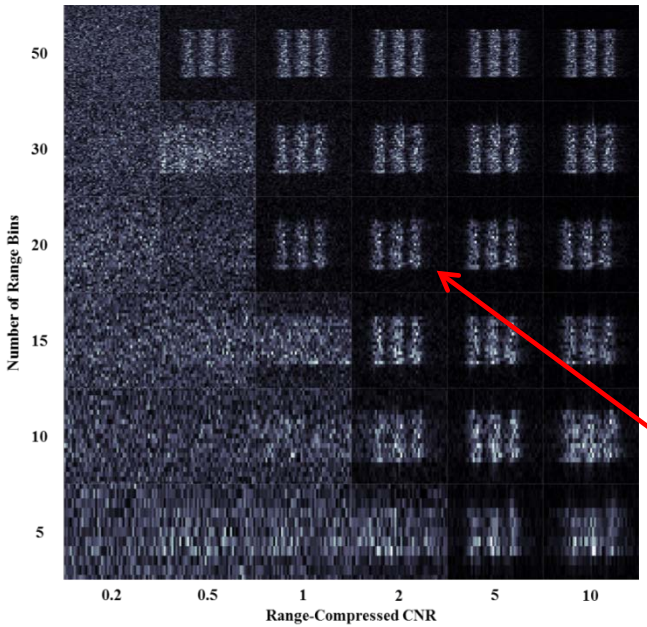


Reconstructed images with the same CNR per range bin

Autofocus Converging

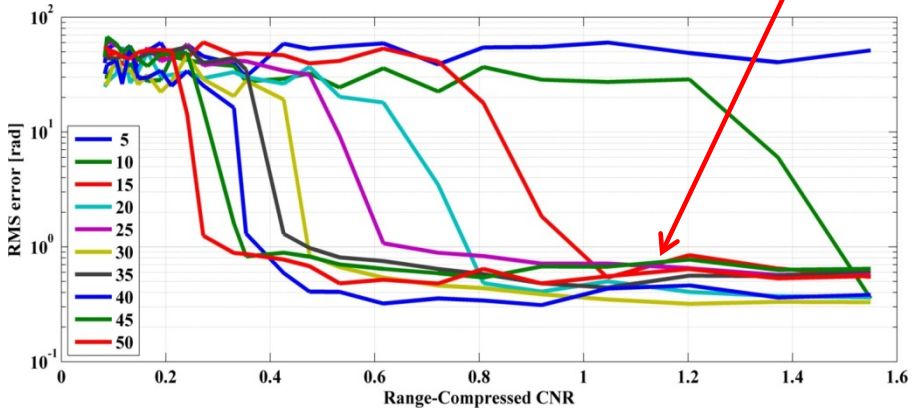


**Verified baseline PGA autofocus requires a CNR~1 for 15-20 range bins**

# Maximum a Posteriori (MAP) Autofocus

- For MAP autofocus, we assume that the main contribution to the phase is due to piston phase and that is normally distributed with mean 0 and covariance *H*.
- The estimate of the piston phase is obtained by minimizing a cost function

$$\hat{\varphi}^{MAP}(m) = \arg\ \min\left( \sum_{i=1}^{m} \left| e^{l\left(\hat{\varphi}^{MAP}(i+1) - \hat{\varphi}^{MAP}(i)\right)} - \frac{1}{N}\sum_{k=1}^{N} \bar{g}(k,i+1)\bar{g}^{*}(k,i) \right|^2 + \left\| H^{-1/2}\hat{\varphi}^{MAP} \right\|^2 \right)$$

phase change in $\varphi$ matches phase change in $\bar{g}$

piston consistent with PSD

- MAP applies the piston estimate repeatedly to estimate $\bar{g}(k,m)$ until convergence is obtained.

# MAP Autofocus Initial Results

- PGA estimates piston change from one pulse to the next.
- PGA does not model of what sort of piston time-series is physical.
- MAP reduces hysteresis and reduces RMS error with deceasing SNR .

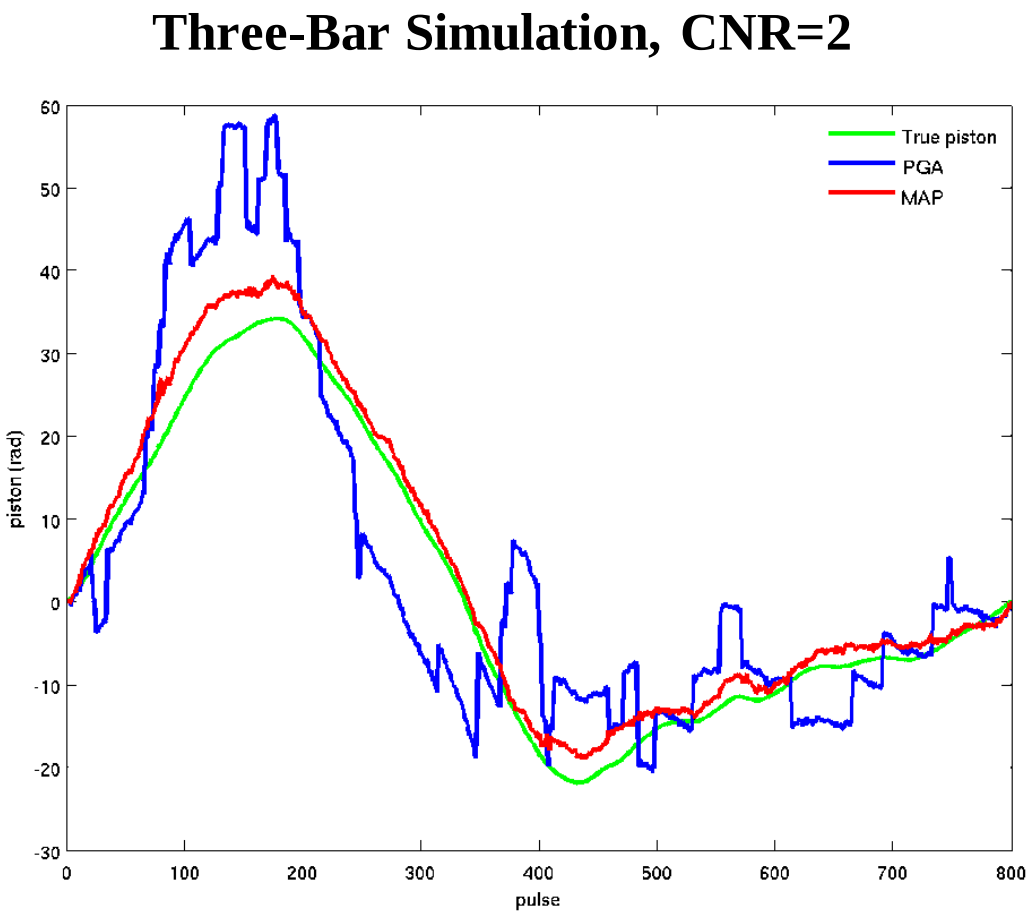


**MAP approaches show promise over PGA approaches**

# JPL Low SNR Laboratory Measurements

From the strongest ball return:

- Photon rate : ~40 ph/s, or ~3ph/pulse/range res. Bin
  - *No FFT windowing for photometry purpose
- CNR per pulse(0.08s): ~1.26 $CNR = \left(P_{object}\right) / P_{bkgrnd}$
- CNR per pulse(0.08s): ~0.26 $CNR = \left(P_{object} - P_{bkgrnd}\right) / P_{bkgrnd}$
- SNR per pulse(0.08s): ~1.22 $SNR = \left(P_{object} - P_{bkgrnd}\right) / \sigma_{bkgrnd}$

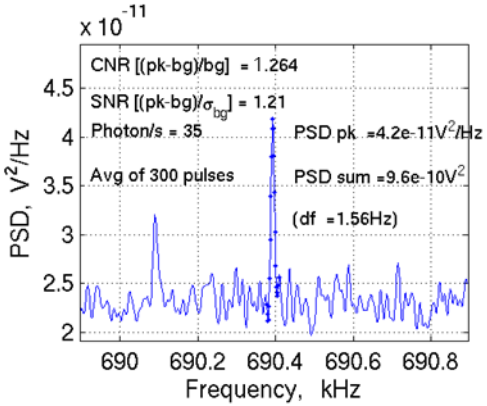


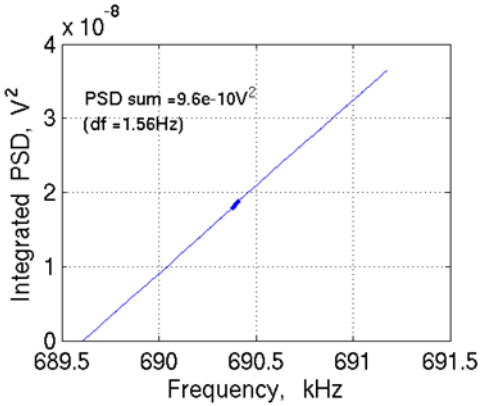


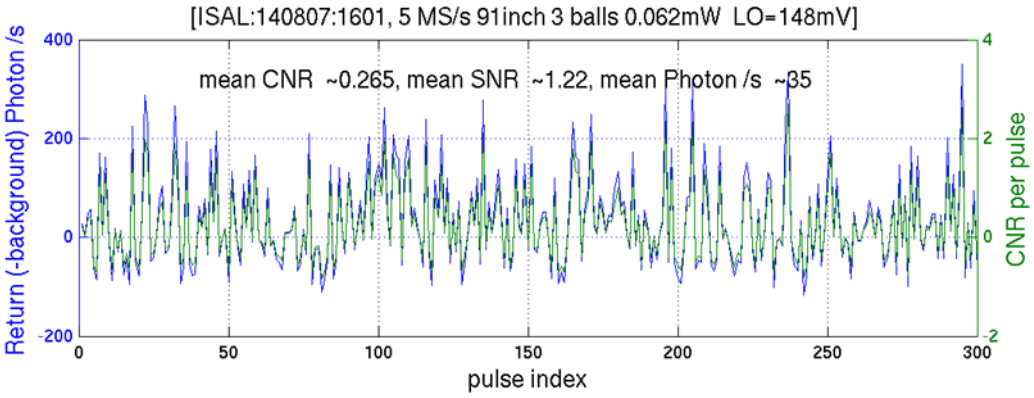


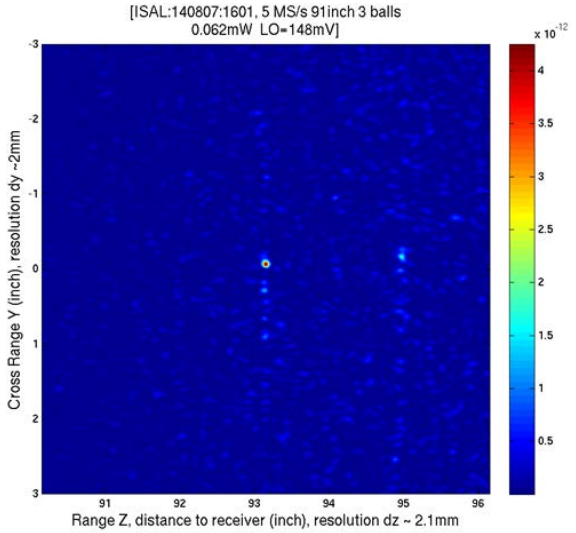


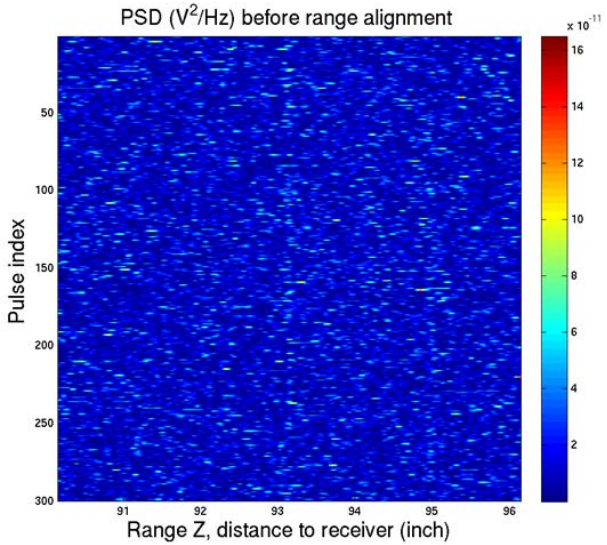

# Tyler 1994 Results for Kolmogorov Atmosphere

- **In the limit of short time intervals, the tracking frequency, $f_T$, is related to the piston time constant, $\tau_p$, by**

$$f_T = 0.331 \ \lambda^{-1} D^{-1/6} \left[ \int dh \, C_n^2(h) \, w(h) \right]^{1/2} = 0.0313 \Big/ \tau_p$$

  - $\lambda$ = wavelength
  - $D$ = aperture diameter
  - $C_n^2$ = Refractive index structure constant profile with height ($h$)
  - $w(h)$ = wind profile with height ($h$)

# Maui 3 Model Tracking Frequency Model Validation

- Star data was collected at Maui over a 90 day period from 45°-90° Zenith angle.
- A Shack-Hartmann Wave Front Sensor was used to measure the tracking frequency.
- Over 100 sample data sets were collected and approximately 75% of those data exhibited Kolmogorov statistical behavior.
- Maui3 atmospheric and geophysics wind models can be used for system design and evaluation.

**$f_T$ Probability Distribution measured with AFRL adaptive optics system in Spring 2012**

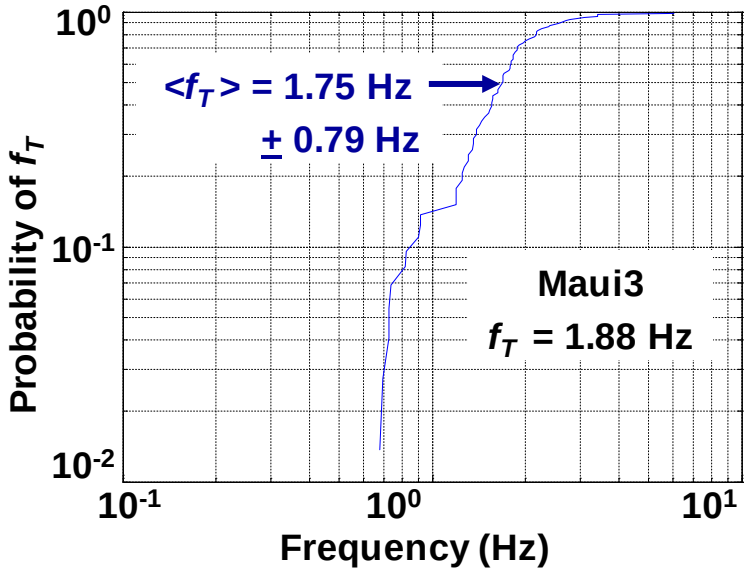


**This process produced values for $f_T$ in excellent agreement with Maui3 model**

**Verified atmospheric constraints on laser chirp period**

# Maui Atmospheric Modeling

- **Atmospheric modeling leverages validated Maui 3 atmospheric model**
  - Model used to evaluate optimal wavelength from 1 to 10 microns.
- **Near IR micron operation has favorable conditions under the assumption of Kolmogorov atmosphere**
  - high transmission >96%
  - benign turbulence $r_0$>50 cm, $f_G$<10 Hz
  - Piston coherence times ~ $\tau_C$ ~30 ms
- **Optimization of ISAL requires understanding of non-Kolmogorov atmosphere in near real-time**

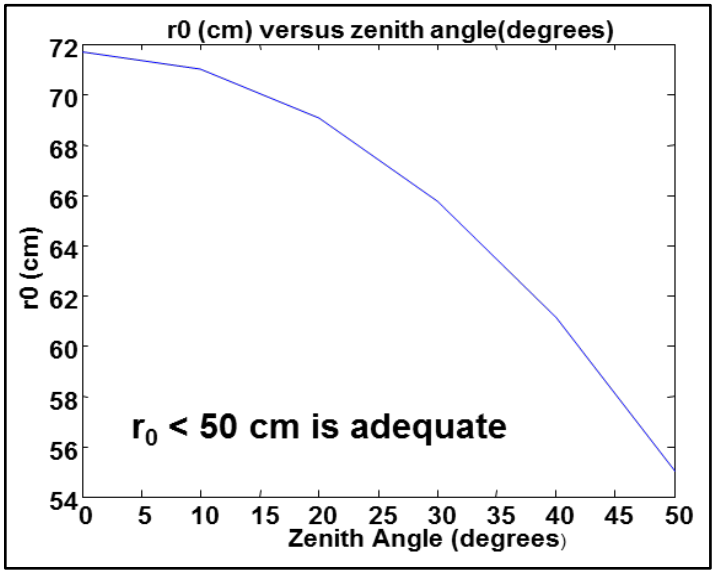


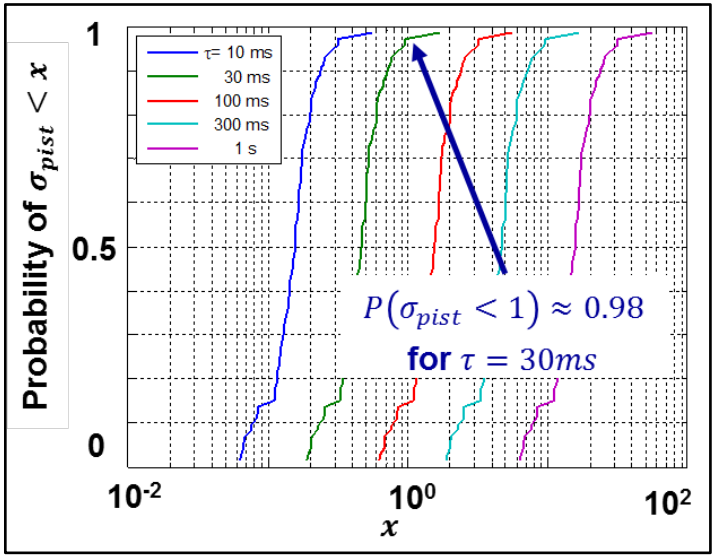

# Piston Time Constant for non-Kolmogorov Atmosphere (1)

**The corresponding piston constant for non-Kolmogorov atmosphere after modifying Tyler analysis for short time intervals**

$$\tau_p = \left[ Q_p \, k^2 D^{p-4} \int C_n^2(z) \, v^2(z) \, dz \right]^{-1/2}$$

$$Q_p = -\frac{2^{-p}\Gamma(p+1)\Gamma\left(-p/2+1\right)}{\Gamma\left(p/2+1\right)\Gamma\left(p/2+2\right)\Gamma\left(p/2+1\right)} \frac{p\,(-p+2)(p+2)}{(-p+1)} \frac{(p-3)}{p-2} \frac{\Gamma(1/2)\,\Gamma(2-p/2)}{\Gamma(5/2-p/2)} \frac{\Gamma(p/2)}{\Gamma(1-p/2)}$$

- **For power-laws of p =[19 20 21 22 23] /6, we get**

  $Q_p$ **=[0.4560 0.9756 1.6674 2.838 5.9929]**

# Tracking Frequency on Centroid Basis for non-Kolmogorov Atmosphere (2)

**The corresponding tracking frequency expression on centroid basis for non-Kolmogorov atmosphere**

$$f_{TG} = (D)^{p/2-2}\,\lambda^{-1/2}\sec^{-1/2}(\psi)\,Q_{tG}\left[\int dh\; C_n^2(h)\;\; v^2\right]^{1/2}$$

$$Q_{tG} = \left[2^{4-p}\,\frac{(p-3)}{(\pi)^2}\,\frac{\Gamma(1/2)}{\Gamma(5/2-p/2)}\,\frac{\Gamma(p-3)\Gamma(3-p/2)}{\Gamma(p/2-1)\Gamma(p/2-1)}\right]^{1/2}$$

**For the 5 non-K exponents, p=[19 20 21 22 23]/6,**

$Q_{tG}$ **= [ 0.3266 0.3314 0.3330 0.3314 0.3266]**

$$f_{tG} = \frac{Q_{tG}}{2\pi\, Q_p^{1/2}}\,\frac{1}{\tau_p}$$

$$= \frac{[\ 0.0780 \quad 0.0533 \quad 0.0408 \quad 0.0313 \quad 0.0215\ ]}{\tau_p}$$

# Tracking Frequency on Z-tilt Basis for non-Kolmogorov Atmosphere (3)

**The corresponding tracking frequency expression on z-tilt basis for non-Kolmogorov atmosphere**

$$f_{tZ} = (D)^{p/2-2} \sec(\psi)^{-1/2} Q_{tZ} \left[ \int dh\, C_n^2(h)\ \ \nu^2 \right]^{1/2}$$

$$Q_{tZ} = \left[ 2^{6-p} \pi^{-3/2} \frac{\Gamma(p-1)\Gamma(3-p/2)}{\Gamma(p/2)\Gamma(2+p/2)} \frac{(p-3)}{\Gamma(5/2-p/2)} \right]^{1/2}$$

**For p=[19 20 21 22 23]/6, $Q_{tZ}$ is calculated as [0.2442 0.3144 0.3505 0.3679 0.3725]**

$$f_{tZ} = \frac{Q_{tZ}}{2\pi\, Q_p^{1/2}} \frac{1}{\tau_p}$$

$$= \frac{[\ 0.0576 \quad 0.0507 \quad 0.0432 \quad 0.0348 \quad 0.0242\ ]}{\tau_p}$$

# Conclusions

- PGA shows excellent baseline performance under low SNR conditions, however, it does not model of what sort of piston time-series is physical.
- MAP approaches show promise over PGA approaches and greatly reduce the RMS error for low SNR conditions.
- JPL laboratory measurements verify the PGA performance evaluated in the full SimISAL simulations.
- The analytical results show that measuring tracking frequency is useful for estimation of piston time constant over short time intervals.
- Maui-3 $C_n^2$ & wind profiles and/or experimental data can be used to get the atmospheric time constants.

# Future Work

- Other MAP approaches will be applied to simulated data in order to reduce the SNR/CNR limit of applicability for autofocus algorithms.
- JPL laboratory measurements will continue to verify/evaluate new autofocus routines at low CNR conditions.
- Analyses for piston time constant over larger time intervals are in progress by modifying Tyler and Fried approaches (non-K atmosphere).
- In general, statistical analysis of larger sets of tracking frequency data will provide a good estimate of site specific average piston characteristics.

**Thank You**

# Back-Up